Continuum Mech. Thermodyn. (2018) 30:1145–1154
https://doi.org/10.1007/s00161-018-0670-6

ORIGINAL ARTICLE

D. J. S. Ferreira · B. N. Bezerra · M. N. Collyer · A. Garcia · I. L. Ferreira

The use of computational thermodynamics for the determination of surface tension and Gibbs–Thomson coefficient of multicomponent alloys

Received: 10 November 2017 / Accepted: 18 April 2018 / Published online: 27 April 2018

Abstract The simulation of casting processes demands accurate information on the thermophysical properties of the alloy; however, such information is scarce in the literature for multicomponent alloys. Generally, metallic alloys applied in industry have more than three solute components. In the present study, a general solution of Butler's formulation for surface tension is presented for multicomponent alloys and is applied in quaternary Al–Cu–Si–Fe alloys, thus permitting the Gibbs–Thomson coefficient to be determined. Such coefficient is a determining factor to the reliability of predictions furnished by microstructure growth models and by numerical computations of solidification thermal parameters, which will depend on the thermophysical properties assumed in the calculations. The Gibbs–Thomson coefficient for ternary and quaternary alloys is seldom reported in the literature. A numerical model based on Powell's hybrid algorithm and a finite difference Jacobian approximation has been coupled to a Thermo-Calc TCAPI interface to assess the excess Gibbs energy of the liquid phase, permitting liquidus temperature, latent heat, alloy density, surface tension and Gibbs–Thomson coefficient for Al–Cu–Si–Fe hypoeutectic alloys to be calculated, as an example of calculation capabilities for multicomponent alloys of the proposed method. The computed results are compared with thermophysical properties of binary Al–Cu and ternary Al–Cu–Si alloys found in the literature and presented as a function of the Cu solute composition.

Keywords Castings · Thermophysical properties · Computational thermodynamics · Ternary Al–Cu–Si alloys · Quaternary Al–Cu–Si–Fe alloys

Communicated by Andreas Öchsner.

D. J. S. Ferreira · B. N. Bezerra · M. N. Collyer · I. L. Ferreira (✉)
Faculty of Mechanical Engineering, Federal University of Pará, UFPA, Augusto Corrêa Avenue 1, Belém, PA 66075-110, Brazil
E-mail: ileao@ufpa.br

D. J. S. Ferreira
E-mail: diegoferreira610@hotmail.com

B. N. Bezerra
E-mail: bnb.norat@gmail.com

M. N. Collyer
E-mail: mr.collyer@hotmail.com

A. Garcia
Department of Manufacturing and Materials Engineering, University of Campinas – UNICAMP, Campinas, SP 13083–860, Brazil
E-mail: amaurig@fem.unicamp.br

1 Introduction

Nucleation, growth and coarsening are phase transformation phenomena that depend on interfacial effects [1]. Considering an isolated solid particle of diameter d, during nucleation it requires a positive energy so to form a surface with high curvature. The Gibbs–Thomson equation shows the effect for the lowering in melting and freezing points, variation in vapor pressure and chemical potential across the forming curved surfaces [2].

Many theoretical solidification growth models have been developed for binary alloys with a view to characterizing important length scales of the phases forming the microstructures, such as cellular and primary (λ_1)/secondary (λ_2) dendrite arm spacings as a function of alloy solute concentration (C_0), solidification thermal parameters and thermophysical properties of the alloy, for both stationary and unsteady heat flow regimes [3–5]. These laws have a thermal and chemical behavior indicatory factor, the Gibbs–Thomson coefficient, which is fundamental for good estimation of the length scale of the as-solidified microstructure, that is, in order to estimate cellular, primary and secondary dendritic arm spacings, the growth models generally depend on the Gibbs–Thomson coefficient of each examined alloy [6–9].

Some studies in the literature have used the analysis of grain boundaries groove shape and the application of numerical methods, to determine the surface tension and the Gibbs–Thomson coefficient for binary and ternary alloys. Gündüz and Hunt developed a numerical model permitting the temperature around a cusp, in alloys having phases with different thermal conductivities, to be calculated. They used the developed approach to compute the surface tension and the Gibbs–Thomson coefficient of binary Al–Cu, Al–Si and Pb–Sn alloys [10]. In a subsequent study, these authors applied their numerical model to determine the solid–liquid surface tension of Al–Mg alloys [11]. Marasli and Hunt used a direct method (by measuring grain boundary cusp) to determine the solid–liquid surface tension and the Gibbs–Thomson coefficient of eutectic Al–$NiAl_3$, Al–$CuAl_2$ and peritectic Al–Ti alloys [12]. Keslioglu and Marasli using the above-mentioned direct method measured the grain boundary groove shapes and, with the help of a numerical method, calculated the Gibbs–Thomson coefficient and the surface tension for solid β (Al–84wt.% Zn) in Al–Zn liquid solutions [13]. Keslioglu et al. determined the Gibbs–Thomson coefficient for solid Al of an Al–Ti solution [14]. Aksöz et al. observed the grain boundary groove shapes of a solid Zn solution (Zn–3.0at.% Al–0.3at.% Bi) in equilibrium with a Zn–Al–Bi eutectic liquid (Zn–12.7 at.%− 1.6 at.%Bi) of a sample quenched in a radial heat flow apparatus. By applying a numerical method, these authors have determined the Gibbs–Thomson coefficient, solid–liquid surface tension and grain boundary energy for the solid Zn solution in equilibrium with a ternary Al–Bi–Zn eutectic liquid [15].

Thermodynamic data applied for surface tension calculation of molten alloys were first carried out by Butler [16] and by the approach of Speiser et al. [17,18]. The method has been later extended so it is able of evaluating the excess Gibbs energy in the bulk of alloys [19]. The surface tension of ternary Ni–Cu–Fe alloys has been described by Brillo et al. [20] based on Tanaka and Lida's work [21]. A thermodynamic–kinetics–solidification model has been proposed by Miettinen, which is able to provide important thermophysical properties data, required for numerically modeling copper alloy castings [22].

Jácome et al. [23] developed a theoretical/numerical approach permitting the Gibbs–Thomson coefficient to be determined for aluminum-based binary alloys. The alloy surface tension was reckoned from the surface tensions and molar volumes of the pure elements by solving Butler's equation, and the necessary excess Gibbs energy was obtained from Thermo-Calc package TCAPI 5 (Thermo-Calc Application Programming Interface v. 5) and TTAL5 (Thermo-Tech Aluminum Database v. 5). These authors have applied the determined Gibbs–Thomson coefficient to cellular and dendritic growth models. In a subsequent study, Jácome et al. [24] extended the previous approach to incorporate the calculation of the Gibbs–Thomson coefficient for ternary Al–Cu–Si alloys.

The aim of this work is to extend the system of equations used to determine the Gibbs–Thomson coefficients for ternary aluminum alloys [24], with a view to permitting the technique to encompass the important case of multicomponent Al-based alloys. The aluminum database used in this paper is the Thermo-Tech TTAL7 (Thermo-Tech Aluminum Database v. 7).

2 Numerical approach

The Gibbs–Thomson effect lowers both the melting and freezing point [1,2]. Considering an isolated solid particle of diameter d in its own liquid, the Gibbs–Thomson equation for the structural melting point depression

can be expressed by [2]:

$$\Delta T_{\mathrm{m}}(d) = T_{\mathrm{m}}^{\mathrm{bulk}} - T_{\mathrm{m}}(d) = \frac{4\,\sigma_{\mathrm{sl}}\,T_{\mathrm{m}}^{\mathrm{bulk}}}{\Delta H \rho_S\, d} \tag{1}$$

where $T_{\mathrm{m}}^{\mathrm{bulk}}$ is the bulk melting temperature of the material, $\Delta T_{\mathrm{m}}(d)$ is the melting point depression [K], σ_{sl} is the solid–liquid interface tension $\left[\mathrm{N\,m^{-1}}\right]$, ΔH is the bulk latent heat of fusion per unit mass $\left[\mathrm{J\,kg^{-1}}\right]$, and ρ_S is the solid phase density $\left[\mathrm{kg\,m^{-3}}\right]$ [2].
Rearranging Eq. 1:

$$\Delta T_m(d) = \frac{4\,\sigma_{\mathrm{sl}}\,T_m^{\mathrm{bulk}}}{\Delta H \rho_S\, d} = \frac{4\,\sigma_{\mathrm{sl}}\,T_m^{\mathrm{bulk}}}{\Delta H_\forall d} = \frac{4\,\sigma_{\mathrm{sl}}}{\Delta S_{\mathrm{sl}}\, d} = \frac{4\,\Gamma}{d} \tag{2}$$

where $\Delta H_\forall$ is latent heat of fusion per unit volume $\left[\mathrm{J\,m^{-3}}\right]$ and ΔS_{Sl} is the solidification entropy heat of fusion per unit volume $\left[\mathrm{J\,m^{-3}\,K^{-1}}\right]$, Γ is the Gibbs–Thomson coefficient expressed in [m K]. Then, the Gibbs–Thomson coefficient can be expressed as,

$$\Gamma = \frac{\sigma_{\mathrm{sl}}\,T_{\mathrm{m}}^{\mathrm{bulk}}}{\Delta H_\forall} \tag{3}$$

Formulations can be found in the literature, which can be used to predict the surface tension of binary and ternary alloys, which are based on the method proposed by Butler [16,19,25,26]. In the case of multicomponent alloys, a general set of equations can be derived as follows:

$$\sigma = \sigma_{SV} + \frac{RT}{A_{SV}} \ln\left[\frac{1-\sum_{i=1}^{n} X_{SLi}^{S}}{1-\sum_{i=1}^{n} X_{SLi}^{B}}\right] + \frac{1}{A_{SV}}\left[\bar{G}_{SV}^{E,S}\left(T, X_{SL1}^{S}, X_{SL2}^{S}, \ldots, X_{SLn}^{S}\right) - \bar{G}_{SV}^{E,B}\left(T, X_{SL1}^{B}, X_{SL2}^{B}, \ldots, X_{SLn}^{B}\right)\right] \tag{4a}$$

$$\sigma = \sigma_{SL1} + \frac{RT}{A_{SL1}} \ln\left[\frac{X_{SL1}^{S}}{X_{SL1}^{B}}\right] + \frac{1}{A_{SL1}}\left[\bar{G}_{SL1}^{E,S}\left(T, X_{SL1}^{S}, X_{SL2}^{S}, \ldots, X_{SLn}^{S}\right) - \bar{G}_{SL1}^{E,B}\left(T, X_{SL1}^{B}, X_{SL2}^{B}, \ldots, X_{SLn}^{B}\right)\right] \tag{4b}$$

$$\sigma = \sigma_{SL2} + \frac{RT}{A_{SL2}} \ln\left[\frac{X_{SL2}^{S}}{X_{SL2}^{B}}\right] + \frac{1}{A_{SL2}}\left[\bar{G}_{SL2}^{E,S}\left(T, X_{SL1}^{S}, X_{SL2}^{S}, \ldots, X_{SLn}^{S}\right) - \bar{G}_{SL2}^{E,B}\left(T, X_{SL1}^{B}, X_{SL2}^{B}, \ldots, X_{SLn}^{B}\right)\right] \tag{4c}$$

$$\sigma = \sigma_{SLn} + \frac{RT}{A_{SLn}} \ln\left[\frac{X_{SLn}^{S}}{X_{SLn}^{B}}\right] + \frac{1}{A_{SLn}}\left[\bar{G}_{SLn}^{E,S}\left(T, X_{SL1}^{S}, X_{SL2}^{S}, \ldots, X_{SLn}^{S}\right) - \bar{G}_{SLn}^{E,B}\left(T, X_{SL1}^{B}, X_{SL2}^{B}, \ldots, X_{SLn}^{B}\right)\right] \tag{4d}$$

In Eq. 4, (R) is the gas constant $[\mathrm{J\,mol^{-1}\,K^{-1}}]$, (σ_{SV}) and (σ_{SLi}) are the surface tension $[\mathrm{N\,m^{-1}}]$ of solvent and solutes, respectively. (A_{SV}) and (A_{SLi}) are the molar surface areas in a monolayer of pure liquid $[\mathrm{m^2}]$ for solvent and solutes, and (X_{SV}) and (X_{SLi}) are the molar fractions of solvent and alloy compounds at the surface and bulk phases, and these two latter variables are interrelated by the expressions $X_{SV}^{S} + \sum_{\mathrm{i}=1}^{n} X_{SLi}^{S} = 1$ and $X_{SV}^{B} + \sum_{i=1}^{n} X_{SLi}^{B} = 1$, respectively. $\bar{G}^{E,S}\left(T, X_{SL1}^{S}, X_{SL2}^{S}, \ldots, X_{SLn}^{S}\right)$ and $\bar{G}^{E,B}\left(T, X_{SL1}^{B}, X_{SL2}^{B}, \ldots, X_{SLn}^{B}\right)$ are the partial excess Gibbs energies of solvent and alloy components in the surface and bulk phases. Excess Gibbs energies are functions of (T) and molar fraction of alloy components in [J mol^{-1}]. Equations 4a–4d correlate the surface tension of the given solution to the properties of pure metals, as well as to the surface area of the metallic monolayer and to the thermodynamic activity of the components in the surface and bulk phases. The molar surface areas are calculated as:

$$A_{SV} = L_0\,\mathrm{N}^{1/3}\,V_{SV}^{2/3} \tag{5a}$$

$$A_{SL1} = L_0\,\mathrm{N}^{1/3}\,V_{SL1}^{2/3} \tag{5b}$$

$$A_{SL2} = L_0 \, \mathrm{N}^{1/3} \, V_{SL2}^{2/3} \tag{5c}$$

$$A_{SLn} = L_0 \, \mathrm{N}^{1/3} \, V_{SLn}^{2/3} \tag{5d}$$

In the set of Eq. 5, N is the Avogadro's number, V is the molar volume [m^3], and L_0 is a geometrical factor for liquid metals assuming close packed structures, which is set to 1.091 [19,25,26]. In the case of multicomponent alloys, the relationship between excess Gibbs energy in the bulk and in the surface phases, based on Gasior's approach [26–29], is

$$\bar{G}^{E,S}\left(T, X_{SL1}^{S}, X_{SL2}^{S}, \ldots, X_{SLn}^{S}\right) = \beta \bar{G}_{E,B}\left(T, X_{SL1}^{B}, X_{SL2}^{B}, \ldots, X_{SLn}^{B}\right) \tag{6}$$

where β is a parameter corresponding to the ratio of the coordination number Z of the surface phase and that of the bulk phase, $\beta = \frac{Z^S}{Z^B}$ and is assumed to be equal to 0.83 for liquid metals. Tanaka e Lida [21] and Speiser et al. [17,18], considering the following equations,

$$\bar{G}_A^{E,\,S}\left(T, N_B^S\right) = \frac{Z^S}{Z^B} \cdot \bar{G}_A^{E,\,B}\left(T, N_B^S\right) \tag{7a}$$

$$\bar{G}_B^{E},\, S\left(T, N_B^S\right) = \frac{Z^S}{Z^B} \cdot \bar{G}_B^{E,\,B}\left(T, N_B^S\right) \tag{7b}$$

and assumed the value of $\beta = \frac{Z^S}{Z^B} = \frac{9}{12} = \frac{3}{4}$. On the other hand, Kasama et al. [29] proposed that the coordination ratio should be $\beta = \frac{Z^S}{Z^B} \sim 1$. Hoar and Melford [25] have considered the coordination ratio varying between $\frac{1}{2}$ and $\frac{3}{4}$, to be appropriate to deal with liquid Pb–Sn and Pb–In alloys. Hajra et al. [30,31] and Lee et al. [32,33] also assumed $\beta = \frac{Z^S}{Z^B} = \frac{3}{4}$. Tanaka et al. [34] using a thermodynamics database to evaluate the surface tension of molten alloys and salt mixtures, by analyzing the equilibrium between surface and bulk phases, they stated that by plotting the surface tension (σ_x) against the ratio of heat formation and phase molar surface area $\left(\frac{\Delta H_x}{A_X}\right)$, that is,

$$\sigma_x = \left(1 - \frac{Z^S}{Z^B}\right) \frac{\Delta H_x}{A_X} \tag{8}$$

the coordination ratio number could not be satisfied neither by $\left(\frac{Z^S}{Z^B}\right)_{\text{metal}} = \frac{3}{4}$ nor by $\left(\frac{Z^S}{Z^B}\right)_{\text{salt}} = \frac{5}{6}$. They have introduced the parameter $\beta = \frac{Z^S}{Z^B}$, and based on their calculations, they obtained $\beta_{\text{metal}} = 0.83$ and $\beta_{\text{molten salts}} = 0.94$ for pure liquid metals and pure molten salts, respectively. These authors have then extrapolated the application of these values for liquid alloys as well as for molten salt mixtures.

Excess Gibbs energies in the bulk phases are calculated directly from Thermo-Calc and Thermo-Tech aluminum and may be obtained from the following thermodynamic relationships:

$$\bar{G}_{SV}^{E,B}\left(T, X_{SL1}^{B}, X_{SL2}^{B}, \ldots, X_{SLn}^{B}\right) = \bar{G}_{SV}^{E,B}\left(T, X_{SL1}^{B}, X_{SL2}^{B}, \ldots, X_{SLn}^{B}\right) - \sum_{i=1}^{n}\left[X_{SLi}^{B} \frac{\partial \bar{G}_{SV}^{E,B}\left(T, X_{SL1}^{B}, X_{SL2}^{B}, \ldots, X_{SLn}^{B}\right)}{\partial X_{SLi}^{B}}\right] \tag{9a}$$

$$\bar{G}_{SL1}^{E,B}\left(T, X_{SL1}^{B}, X_{SL2}^{B}, \ldots, X_{SLn}^{B}\right) = \bar{G}_{SV}^{E,B}\left(T, X_{SL1}^{B}, X_{SL2}^{B}, \ldots, X_{SLn}^{B}\right) - \left[1 - \sum_{i=1}^{n} X_{SLi}^{B}\right] \frac{\partial \bar{G}_{SV}^{E,B}\left(T, X_{SL1}^{B}, X_{SL2}^{B}, \ldots, X_{SLn}^{B}\right)}{\partial X_{SL1}^{B}} \tag{9b}$$

$$\bar{G}_{SL2}^{E,B}\left(T, X_{SL1}^{B}, X_{SL2}^{B}, \ldots, X_{SLn}^{B}\right) = \bar{G}_{SV}^{E,B}\left(T, X_{SL1}^{B}, X_{SL2}^{B}, \ldots, X_{SLn}^{B}\right) - \left[1 - \sum_{i=1}^{n} X_{SLi}^{B}\right] \frac{\partial \bar{G}_{SV}^{E,B}\left(T, X_{SL1}^{B}, X_{SL2}^{B}, \ldots, X_{SLn}^{B}\right)}{\partial X_{SL2}^{B}} \tag{9c}$$

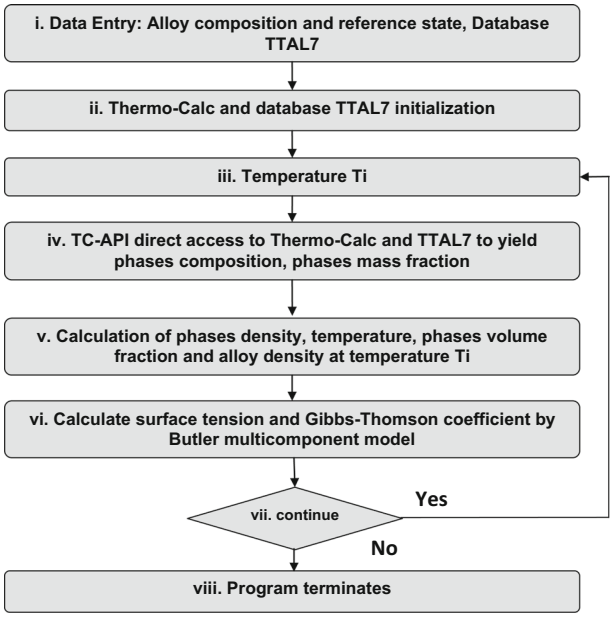

Fig. 1 Solution scheme for determination of alloy density, surface tension and Gibbs–Thomson coefficient for multicomponent alloy by calling Thermo-Calc and TTAl7 API through a C language program

$$\bar{G}^{E,B}_{SLn}\left(T, X^B_{SL1}, X^B_{SL2}, \ldots, X^B_{SLn}\right) = \bar{G}^{E,B}_{SV}\left(T, X^B_{SL1}, X^B_{SL2}, \ldots, X^B_{SLn}\right) - \left[1 - \sum_{i=1}^{n} X^B_{SLi}\right] \frac{\partial \bar{G}^{E,B}_{SV}\left(T, X^B_{SL1}, X^B_{SL2}, \ldots, X^B_{SLn}\right)}{\partial X^B_{SLn}} \quad (9d)$$

The solution scheme applied in this work, shown in Fig. 1, has a similar structure of those proposed by Nascimento et al. [35] to calculate the alloy density of ternary alloys and by Jácome et al. [36] to compute surface tension of ternary aluminum-based alloys. This solution scheme is herewith extended to encompass the calculation the surface tension of multicomponent alloys and can be summarized by the following steps:

1. In the data entry routine, the user must provide the following setup variables: thermodynamics database (TTAL7, TCMP2), composition in weight percent for each alloy compound (Cu, Si, Fe, Ag, Zn, Mg, ...) and reference state ($T = 1000\,\text{K}$, $P = 101325\,\text{Pa}$ and $N = 1\,\text{mol}$);
2. Initialization of the Thermo-Calc software from TCAPI 5 interface and database provided in step i;
3. Calculation of the liquidus temperature for the specific alloy composition provided in step i;
4. Calculation of phases mass fractions and the phases compositions;
5. Calculation of the volume data for each phase, which is not normally present in the thermodynamics databases, then compute phases densities for a thermodynamics condition of initial formation of the solid phase(s) in a temperature immediately below the liquidus temperature;
6. In the case of aluminum alloys, by using the Scheil simulation from Thermo-Calc module, the latent heat in [J kg^{-1}] is calculated and the solidification entropy is determined. By solving Butler's system of equation for surface tension and by applying Eq. (1), the Gibbs–Thomson coefficient is numerically determined;
7. Program will continue if the alloy provided in step i has a composition range; otherwise, it goes to step 8;
8. The routine de-initializes Thermo-Calc database and the TCAPI interface sets dynamic allocated memory free and terminates the execution.

3 Results and discussion

With a view to permitting binary, ternary quaternary alloys to be compared, some thermophysical properties used can be found in Table 1 [23].

Table 1 Thermophysical properties of alloys components [23]

Properties	Unit	Value
Aluminum molar volume (V_{Al})	$m^3\ mol^{-1}$	1.13×10^{-05}
Copper molar volume (V_{Cu})	$m^3\ mol^{-1}$	7.43×10^{-06}
Silicon molar volume (V_{Si})	$m^3\ mol^{-1}$	1.205×10^{-05}
Iron molar volume (V_{Fe})	$m^3\ mol^{-1}$	7.09×10^{-06}
Aluminum surface tension (σ_{Al})	$N\ m^{-1}$	0.9140
Copper surface tension (σ_{Cu})	$N\ m^{-1}$	1.2900
Silicon surface tension (σ_{Si})	$N\ m^{-1}$	0.7330
Iron surface tension (σ_{Fe})	$N\ m^{-1}$	1.8060
Parameter (L_0)		1.090
Coordination number ratio (β)		0.83
Gas constant (R)	$J\ mol^{-1}\ K^{-1}$	8.31451

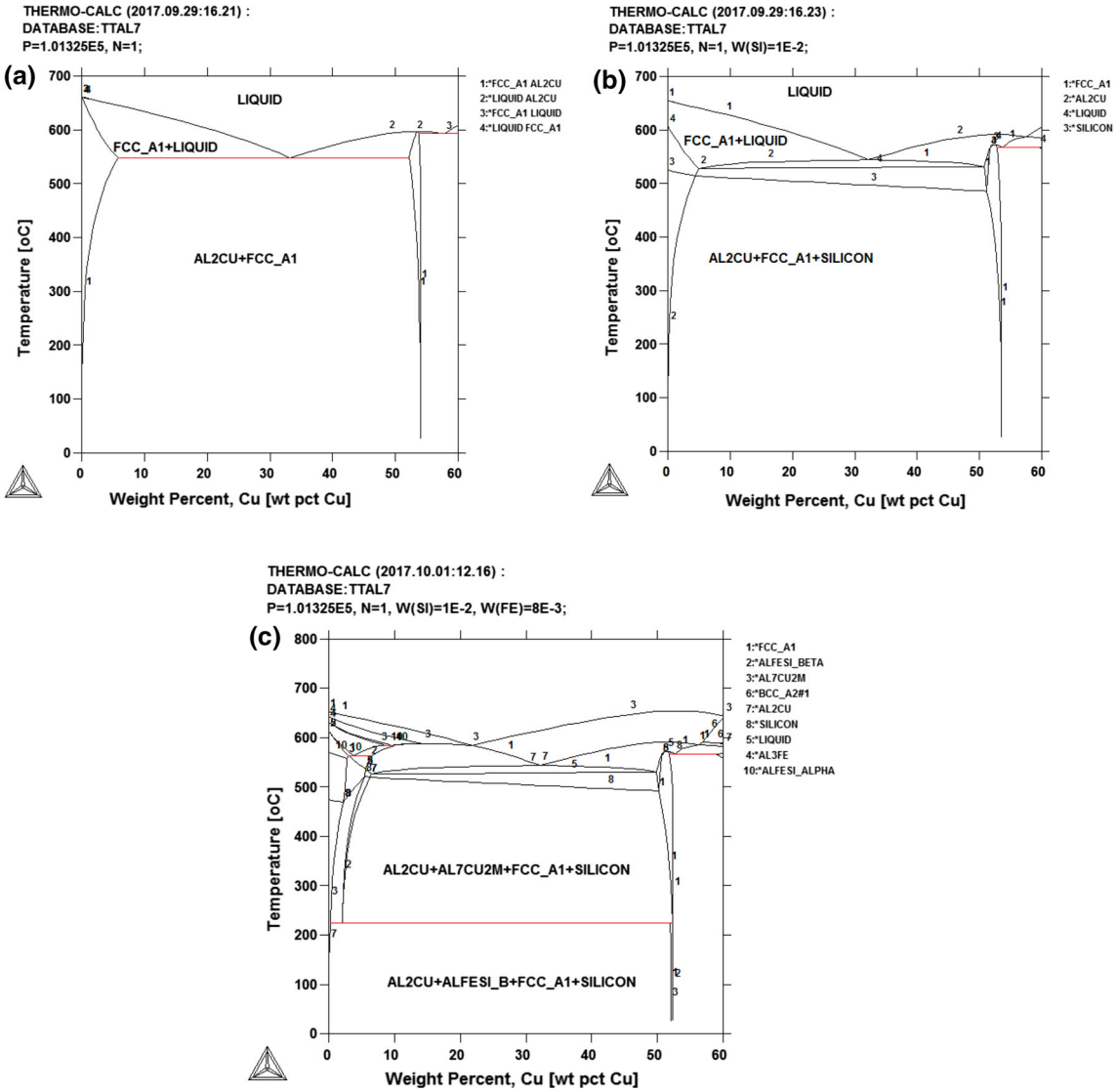

Fig. 2 Al–Cu binary phase diagram (**a**), Al–Cu–1wt pct Si (**b**) and Al–Cu–1wt pct Si–0.8wt pct Fe (**c**) pseudo-binary phase diagrams

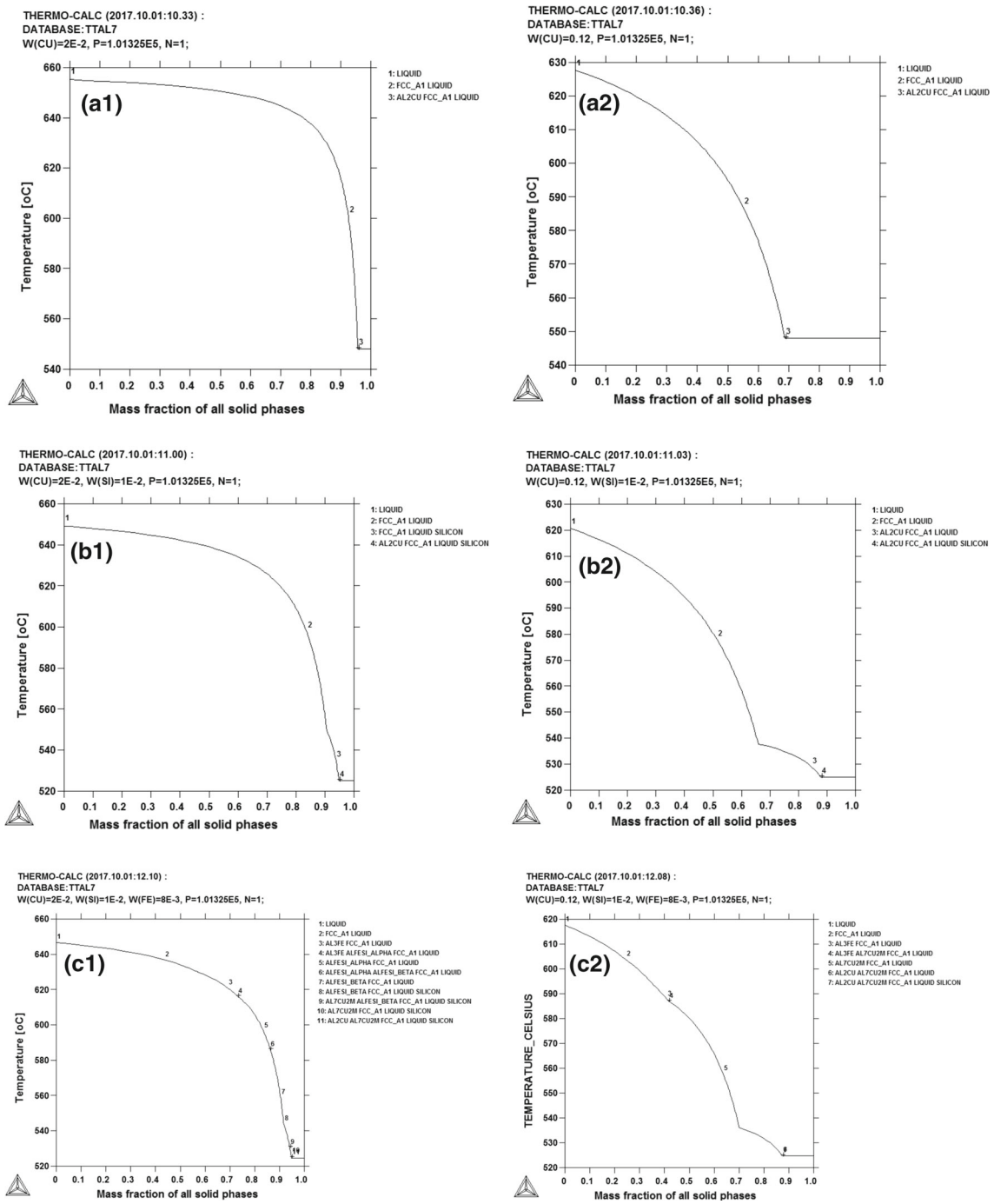

Fig. 3 Scheil's simulations of Al-(2 and 12) wt pct Cu, Al-(2 and 12)wt pct Cu–1wt pct Si, and finally, Al-(2 and 12)wt pct Cu–1wt pct Si–0.8wt pct Fe

Figure 2 shows phase diagrams calculated by the Thermo-Calc software: (A) binary phase diagram of Al–Cu; (B) Al–Cu–1wt pct Si and (C) Al–Cu–1wt pct Si–0.8wt pct Fe pseudo-binary phase diagrams. In Fig.2a only eutectic (AL2CU) and Al-rich phase (FCC_A1) can be found as stable solid phases. In Fig. 2b, metallic silicon phase is precipitated for any temperature below its solubility curve 3. Then, in the solid region three phases can be found (AL2CU, FCC_A1 and SILICON). In Fig. 2c, besides the prior mentioned phases, the AL7CU2M phase can also be found, also known as AL7CU2FE, which transforms into the ALFESI_β phase for temperatures below, approximately $T = 223{,}22\,^{\circ}\mathrm{C}$.

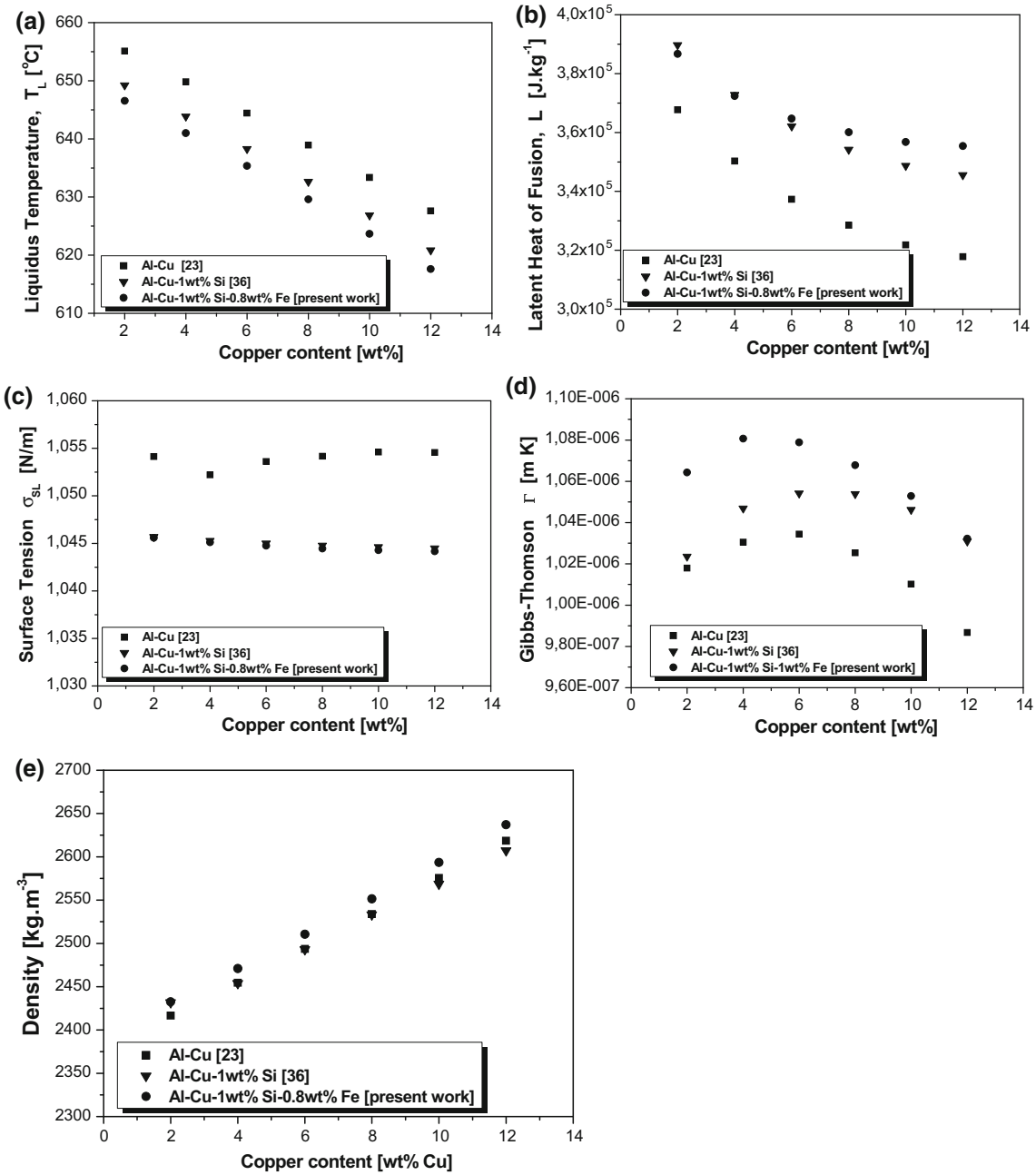

Fig. 4 Comparison between thermophysical properties as a function of composition of binary Al–Cu, ternary Al–Cu-1wt%Si and quaternary Al–Cu–1wt%Si–0.8wt%Fe alloys: **a** liquidus temperature, **b** latent heat of fusion **c** surface tension, **d** Gibbs–Thomson coefficient and **e** density as a function of Cu content

Figure 3 depicts Scheil's simulations of Al-(2 and 12)wt pct Cu, Al-(2 and 12)wt pct Cu–1wt pct Si, and finally, Al-(2 and 12)wt pct Cu–1wt pct Si–0.8wt pct Fe. The same phases of the equilibrium condition also appear in the non-equilibrium simulations. The Al7CU2M (AL7CU2FE) phase is decomposed by solid-state reaction into ALFESI_β.

For comparison purposes, Fig. 4 shows the evolution of properties of binary Al–Cu, ternary Al–Cu–1wt%Si and quaternary Al–Cu–1wt%Si–Fe alloys as a function of Cu concentration. Figure 4a shows the evolution of *liquidus* temperatures of Al–Cu and Al–Cu–1wt%Si and Al–Cu–1wt%Si–Fe Al alloys, which decrease with the increase in Cu content. It can be seen that, despite being essentially constant with the increase in the Cu content, the surface tension for binary alloys is higher than the corresponding values observed for ternary alloys

and quaternary alloys (Fig. 4c). An opposite behavior can be observed for the latent heat (L) evolution with the Cu content of the alloys, as shown in Fig. 4b, i.e., L decreases with the increase in the alloy Cu content, and the ternary and quaternary alloys have always higher values of L when compared with those of the binary Al–Cu alloy having a same Cu content. Figure 3d depicts the Gibbs Thomson coefficient as a function of the Cu composition of the alloys, which has been calculated by Eq. 1. It can be seen that Γ varies significantly with the Cu content for any alloy examined. For binary alloys, it is a common practice in the literature to assume a constant value for Γ based on the properties of the solvent, for the calculation of microstructural parameters such as the dendritic spacing [36]. The evolution of the Gibbs–Thomson coefficient with the alloys composition depicted in Fig. 4d gives clear indication that such procedure can induce significant errors. Figure 4e shows density of binary, ternary and quaternary alloys as a function of Cu content, which have been calculated as previously proposed by Nascimento et al. [35]. A difference of 7.85% in density can be observed between the lowest and the highest concentration of quaternary alloys, giving indications of the importance of accurately determining the thermophysical properties in the simulation of castings.

4 Conclusion

An approach for calculating surface tension and Gibbs–Thomson coefficient for multicomponent alloys has been proposed. A comparison between properties of Al–Cu, Al–Cu–1wt%Si and Al–Cu–1wt Si–0.8wt% Fe alloys has been carried out. It was shown that the Gibbs–Thomson coefficient varies significantly with the Cu content of the alloy for binary, ternary and quaternary Al–Cu-based alloys examined. The present results make clear that accurate thermophysical properties for specific alloys compositions are absolutely necessary in order to permit reliable evaluations of surface tension and Gibbs–Thomson coefficient, which are fundamental to the reliability of predictions furnished by microstructure growth models and by numerical computations of solidification thermal parameters. By applying the proposed general formulation, the only limit to calculations with multicomponent alloys is that provided by the available thermodynamics database, which must provide data such as liquidus temperature, latent heat, specific heat, phase density and alloy density.

Acknowledgements The authors acknowledge the financial support provided by FAPERJ (The Scientific Research Foundation of the State of Rio de Janeiro), CAPES and CNPq (The Brazilian Research Council).

References

1. Perez, M.: Gibbs–Thomson effects in phase transformations. Scr. Mater. **52**, 709–712 (2005)
2. Zinn, T., Willner, L., Lund, R.: Nanoscopic confinement through self-assembly: crystallization within micellar cores exhibits simple Gibbs–Thomson behavior. Phys. Rev. Lett. **113**(238305), 238305 (2014)
3. Bouchard, D., Kirkaldy, J.S.: Prediction of dendrite arm spacings in unsteady and steady-state heat flow of unidirectionally solidified binary alloys. Metall. Mater. Trans. B **28B**, 651–663 (1997)
4. Hunt, J.D., Lu, S.Z.: Numerical modeling of cellular/dendritic array growth: spacing and structure predictions. Metall. Mater. Trans. A **27**, 611–623 (1996)
5. Rappaz, M., Boettinger, W.J.: On dendritic solidification of multicomponent alloys with unequal liquid diffusion coefficients. Acta Mater. **47**, 3205–3219 (1999)
6. Kurz, W., Fisher, J.D.: Dendrite growth at the limit of stability: tip radius and spacing. Acta Metall. **29**, 11–20 (1981)
7. Trivedi, R.: A comparison of theory and experiments. Metall. Mater. Trans. **15A**, 977–982 (1984)
8. Goulart, P.R., Cruz, K.S., Spinelli, J.E., Ferreira, I.L., Cheung, N., Garcia, A.: Cellular growth during transient directional solidification of hypoeutectic Al–Fe alloys. J. Alloys Compd. **470**, 589–599 (2009)
9. Costa, T.A., Moreira, A.L., Moutinho, D.J., Dias, M., Ferreira, I.L., Spinelli, J.E., Rocha, O.L., Garcia, A.: Growth direction and Si alloying affecting directionally solidified structures of Al–Cu–Si alloys. Mater. Sci. Technol. **31**, 1103–1112 (2015)
10. Gündüz, M., Hunt, J.D.: The measurement of solid-liquid surface energies in the Al–Cu, Al–Si and Pb–Sn systems. Acta Metall. **33**, 1651–1672 (1985)
11. Gündüz, M., Hunt, J.D.: Solid–liquid surface energy in the Al–Mg system. Acta Metall. **37**, 1839–1845 (1989)
12. Marasli, N., Hunt, J.D.: Solid-liquid surface energies in the Al-$CuAl_2$, Al-$NiAl_3$ and Al–Ti systems. Acta Mater. **44**, 1085–1096 (1996)
13. Keslioglu, K., Marasli, N.: Solid–liquid interfacial energy of the eutectoid β phase in the Al–Zn eutectic system. Mater Sci. Eng. A **369**, 294–301 (2004)
14. Keslioglu, K., Gunduz, M., Kaya, H., Çadirli, E.: Solid–liquid interfacial energy in the Al–Ti system. Mater. Lett. **58**, 3067–3073 (2004)
15. Aksöz, S., Ocak, Y., Marasli, N., Keslioglu, K.: Dependency of the thermal and electrical conductivity on the temperature and composition of Cu in the Al based Al–Cu alloys. Exp. Therm. Fluid Sci. **35**, 395–404 (2011)
16. Butler, J.A.V.: The thermodynamics of the surfaces of solutions. Proc. R. Soc. A **135**, 348–375 (1932)
17. Speiser, R., Poirier, D.R., Yeum, K.S.: Surface tension of binary liquid alloys. Scr. Metall. **21**, 68–692 (1987)

18. Yeum, K.S., Speiser, R., Poirier, D.R.: Estimation of the surface tensions of binary liquid alloys. Metall. Trans. **20B**, 693–703 (1989)
19. Picha, R., Vrestal, J., Kroupa, A.: Prediction of alloy surface tension using a thermodynamic database. CALPHAD **28**, 141–146 (2004)
20. Brillo, J., Egry, I., Matsushita, T.: Density and surface tension of liquid ternary Ni–Cu–Fe alloys. Int. J. Thermophys. **27**, 1778–1791 (2006)
21. Tanaka, T., Lida, T.: Application of a thermodynamic database to the calculation of surface. Tension for iron-base liquid alloys. Steel Res. **65**, 21–28 (1994)
22. Miettinen, J.: Thermodynamic–kinetic model for the simulation of solidification in binary copper alloys and calculation of thermophysical properties. Comput. Mater. Sci. **36**, 367–380 (2006)
23. Jácome, P.A.D., Landim, M.C., Garcia, A., Furtado, A.F., Ferreira, I.L.: The application of computational thermodynamics and a numerical model for the determination of surface tension and Gibbs–Thomson coefficient of aluminum based alloys. Thermochim. Acta **523**, 142–149 (2011)
24. Jácome, P.A.D., Moutinho, D.J., Gomes, L.G., Garcia, A., Ferreira, A.F., Ferreira, I.L.: The application of computational thermodynamics for the determination of surface tension and Gibbs–Thomson coefficient of aluminum ternary alloys. Mater. Sci. Forum **730–732**, 871–876 (2013)
25. Hoar, T.P., Melford, D.A.: The surface tension of binary liquid mixtures: lead + tin and lead + indium alloys. Trans. Faraday Soc. **53**, 315–326 (1957)
26. Gasior, W., Moser, Z., Pstrus, J., Krzyzak, B., Fitzner, K.: Surface tension and thermodynamic properties of liquid Ag–Bi solutions. J. Phase Equilib. **24**, 40–49 (2003)
27. Tanaka, T., Hack, K., Lida, T., Hara, S.: Application of thermodynamic databases to the evaluation of surface tension of molten alloys, salt mixture and oxide mixtures. Z. Metallkd. **87**, 380–389 (1996)
28. Tanaka, T., Hack, K., Hara, S.: Use of thermodynamic data to determine surface tension and viscosity of metallic alloys. MRS Bull. **24**, 45–51 (1999)
29. Kasama, A., Inui, T., Morita, Z.: Measurements of surface tension of liquid Ag–Au and Cu–(Fe, Co, Ni) binary alloys. Jpn. Inst. Met. **42**, 1206–1212 (1978)
30. Hajra, J.P., Lee, H.K., Frohberg, M.G.Z.: Calculation of surface tension of liquid binary systems from the data of the pure components and the thermodynamic infinite dilution values. Z. Metallkde. **82**, 603–608 (1991)
31. Hajra, J.P., Frohberg, M.G.Z., Lee, H.K.: Calculation of surface tension of liquid binary systems from the data of the pure components and the thermodynamic infinite dilution values. Z. Metallkde. **82**, 603–608 (1991)
32. Lee, H.K., Hajra, J.P., Frohberg, M.G.Z.: Calculation of the surface tensions in liquid ternary metallic systems. Z. Metallkde. **83**, 638–643 (1992)
33. Lee, H.K., Frohberg, M.G.Z., Hajra, J.P.: The determination of the surface tensions of liquid iron, nickel and iron–nickel alloys using the electromagnetic oscillating droplet technique. Steel Res. **64**, 191–196 (1993)
34. Tanaka, T., Kitamura, T.: Evaluation of surface tension of molten ionic mixtures, I. A. Back. ISIJ Int. **46**, 400–406 (2006)
35. Nascimento, F.C., Paresque, M.C.C., de Castro, J.A., Jácome, P.A.D., Garcia, A., Ferreira, I.L.: Application of computational thermodynamics to the determination of thermophysical properties as a function of temperature for multicomponent Al-based alloys. Thermochim. Acta **619**, 1–7 (2015)
36. Jácome, P.A.D., Fernandes, M.T., Garcia, A., Ferreira, A.F., Castro, J.A., Ferreira, I.L.: Application of computational thermodynamics to the evolution of surface tension and Gibbs–Thomson Coefficient during multicomponent aluminum alloy solidification. Mater. Sci. Forum **869**, 416–422 (2016)